

An Analysis of the Fractional Distribution of the Substantial Composition of Limonitic Nickel Ore from Punta Gorda, Moa, Holguin, Cuba*

¹G. Agyei, ²A. H Flores and ²A.R Purón
¹University of Mines and Technology, Tarkwa, Ghana
²Instituto Superior Minero Metalurgico de Moa, Cuba

Agyei, G., Hernandez, A.F. and Rojas, A. P. (2018), "Analysis of the Fractional Distribution of the Substantial Composition of Limonitic Nickel Ore from Punta Gorda, Moa, Holguin, Cuba", *Ghana Mining Journal*, Vol. 18, No. 2, pp. 9 - 20.

Abstract

This paper evaluates the mass and content distribution of the lateritic ore supplied to the Caron process in Moa, Cuba. The description of the most contrasting physical properties, particle size and magnetic susceptibility with the use of fractional analysis methods was done. The products of fractional analysis were further set to the analytical techniques of X-Ray Fluorescence (XRF), powder X-Ray Diffraction (XRD) and Atomic Absorption to determine the metallic and mineralogical phases. Statistical approaches were also used to validate the distribution functions. As a result of the research, the regularities of mass and content distribution of the following phases were determined: Ni, Co, Fe, Al, Mg, SiO₂, Mn and Cr. In addition, the joint fractional distribution functions that describe the mass and content of the aforementioned physical properties were found; an aspect that may allow for the possibility of identifying the particles according to the physical properties under study. These results may add up to the new knowledge about the possibilities of pre-concentration by elimination of components that do not have metal values of interest in the Caron process.

Keywords: Theory of Separation, Fractional Distribution Function, Laterite, Nickel

1 Introduction

The increase in the cost of current technological processes used to recover nickel due to the high cost of energy and the fluctuations in the price of metals in the market, in the context of the current global financial crisis, have generated various questions from researchers, technologists and investors, on the need to find innovative technological processes, through the beneficiation of the laterite ore. Therefore, it is necessary to review and deepen the knowledge about the contrasts in physical properties of the ore, such as magnetic susceptibility and particles sizes, for possible pre-concentration of useful components.

The nickel ore formed from the weathering of the basic and ultrabasic serpentine rocks of the North-east of Eastern Cuba, constitutes the main raw material obtained from the lateritic profiles of Punta Gorda deposit, Moa, Holguin. It is locally referred to as balance laterite (cut-off grade) of the Caron process for the extraction of nickel and cobalt. The oxide nickel for the Caron process requires an iron content higher than 35%, and the Ni greater than 1% (Vera, 1979). It is taken into account the presence of other metals such as Al, Cr, Co and Mn which can be extracted with a more comprehensive usage; hence, the need to know in more detail, the mineralogical aspects of this lateritic ore.

Ponce and Carrillo (1984) assess the substantial composition, size distribution and magnetic properties of ferronickel ore from the "La Delta" deposit. Later, using a laterite standard sample, Ponce and Carrillo (1988) determine the mineralogical composition, size analysis and electromagnetic fractions over a fairly wide range. They report that the predominant class of the sample is 0.05-0.01 mm and the main phases are goethite-hydrogoethite, clay minerals, magnetites, chromspinel, serpentine group minerals and manganese minerals. The works of (Rodríguez, 1990; Almaguer, 1993, 1996; Rojas, 1995; Beyris, 1997) indicate some contrasts in the concentration of different elements from different zones and different particle sizes. Nickel and iron tend to concentrate in the smallest particles (44 microns) whilst minerals containing cobalt, chromium and manganese are concentrated in intermediate particles between 200 and 20 microns and because of their higher density they can be separated from other silicates and accompanying oxides (Almaguer 1989, 1993, 1995; Rojas, 1995).

Beyris (1997) evaluating the influence of the mineralogical composition of the slurry in thickeners shows that the silicate mineral phases are concentrated in the coarse fractions, whilst the iron oxide mineral phases are enriched in the fine size fractions, corroborating previous results from Beyris and Rojas (1994) for different mining faces. Carthy and Falcón (1985) and Leyva *et al* (1995) report of chromite concentrates from a combined

*Manuscript received October 05, 2018

Revised version accepted December 03, 2018

<https://dx.doi.org/10.4314/gm.v18i2.2>

flowsheet of classification-magnetic separation from the Nicaro oxide nickel deposit. For the balance laterites, Hernández *et al.* (1995) applying a meticulous washing flowsheet, show that in the cyclone classification, the overflow is enriched in iron and nickel and depleted in aluminium and magnesium.

At the end of the 1980s and the beginning of the 2000s, researchers from the Department of Metallurgy of the Instituto Superior Minero Metalurgico de Moa carried out important group of works aimed at the beneficiation of laterites and their tailings with several approaches, which have been summarized in Hernández *et al.*, 1995, 1997, 2000; Beyris, 1997; Coello *et al.*, 1998; Ramírez, 2002; Agyei *et al.* 2010; Agyei and Byris 2011; Hernandez *et al.* 2017;). Hernández (1997) performs a theoretical analysis on the possibility of concentrating the main components of the laterite ore, using the methodological elements provided by Tikhonov (1978, 1984). According to the results, it is possible to increase nickel by 0.08% and decrease the content of aluminium and magnesium by 8.56% and 6.58% respectively for the overflow of hydrocyclone classification.

Beneficiation curves are an efficient way to evaluate the separation of ores whose components differ in a single physical property (density, magnetic susceptibility and others). The contrast index according to Tikhonov (1984), can be expressed in Equation (1) as:

$$I_{const} = \bar{\beta}_{min}^{-1} \int_{\xi_{min}}^{\xi_{max}} |\beta(\xi) - \bar{\beta}_{inc}| \gamma(\xi) d\xi \quad (1)$$

where:

$\gamma(\xi)$ is the mass differential distribution;

$\beta(\xi)$ is the content differential distribution;

(ξ) is the physical property; and

$\bar{\beta}_{inc}$ is the head grade.

Coello *et al.* (1998) state that from Equation (1), it can be seen that ores with different degrees of beneficiability $\gamma(\xi)$ and $\beta(\xi)$ can have the same contrast index, so it is not advisable to use this criterion for complex multicomponent ores, because it can lead to unpredictable mistakes. On the other hand, the classical approach in the investigation of the beneficiability of minerals (beneficiability curve contrast in physical and physico-chemical or other properties) does not provide all the necessary information for technological forecasting and design in the treatment of complex ores. Coello *et al.* (1998), after a rigorous analysis of the previous works,

elaborate on the limitations of using the beneficiability curves for the study of lateritic ores and their tailings, and propose the use of the fractional approach for the following reasons:

- (i) Ore particles differ not by a physical property, which implies the use of different separation properties;
- (ii) Ore particles are bearers not only of a useful mineral, but of several accompanying mineral particles; and
- (iii) The use of the fractional approach by more than one separation property allows to delineate the separation limits of the mineralogical phases present in the low-grade nickel laterite ore.

The functions of mass distribution, $\gamma(\xi)$ and content distribution, $\beta(\xi)$ are simple, indispensable and appropriate means for the description of any ore.

Any other method is deficient or too complex, as in the case of beneficiability curves, where the components differ in more than two physical properties. These distribution functions do not only allow the calculation of the classic indicators of beneficiation, but also the prognosis of the technological indices of any beneficiation arrangement, irrespective of the separation property (Coello *et al.*, 1998).

The revision and understanding about the pre-concentration capabilities of the ochreous laterite constituents are still inadequate; any study concerned with the inclusion of beneficiation unit operations in pre-concentration for improvement in the Caron process, ought to evaluate the fractional distribution of chemical elements in the laterite ore, covering particles within a size range of 8.0 to 0.044 mm.

The scientific problem to be solved is the complexity and the serious methodological limitations in the applicability of the beneficiability curves for the study of the nickel laterite ore and the search of preconcentration alternatives that satisfy the industrial needs for improved technological efficiency of the Caron process at Moa. The objective is to determine the joint fractional integrative-differential distribution functions that describe the substantial composition of the balance laterite according to the size of mineral particles and magnetic susceptibility.

1.2 Theoretical Fundamentals

The objective of beneficiation process is to separate, by contrasting physical or chemical-physical properties, the useful minerals from the

initial ore. This separation occurs according to the physical properties of the particles that make up the feed. The particles with certain characteristics pass to the concentrate while the others remain in the tailings. The beneficiation flowsheet can consider only one physical property (density, size, magnetic susceptibility, etc.) or several of them. It is obvious that the effectiveness can be measured by analysing the initial distribution of the useful component in the raw material and its distribution in the final concentrate.

In a first approach to the problem, the physical property can be expressed using a real variable ρ . The variable can be considered as a random variable, by randomly taking samples of particles and measuring them. The results will be different and random, thus expressing the heterogeneity of the initial ore. If the variable is denoted by ρ , then the probability distribution can be expressed as in Equation (2):

$$\int_{-\infty}^{+\infty} \gamma(\rho) d\rho = \int_{\rho_{\min}}^{\rho_{\max}} \gamma(\rho) d\rho = 1 \quad (2)$$

$$\gamma(\rho_o) = \frac{1}{\Delta\rho} \lim_{\Delta\rho \rightarrow 0} P(\rho_o < \rho < \rho_o + \Delta\rho)$$

The function, γ characterizes the distribution of the particles of the feed ore according to the physical property ρ . The value $\gamma(\rho)d\rho$ expresses the proportion of the fraction $[\rho, \rho + d\rho]$ with respect to the initial mineral (Tikhonov, 1984; King, 2001).

An ideal separator would allow to classify the head grade particles into two groups: if the value of ρ is greater than a given threshold ρ_o or not. When represented by the probability that the particles with physical property pass to the concentrate, the graph for the function of the separator will be similar to Fig. 1.

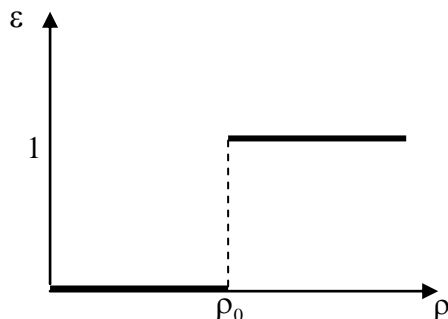


Fig.1 Ideal Separation

However, ideal separators do not exist because classification errors inevitably occur when particles that have to pass to the concentrate report to the tailings and vice versa. That is why the function for the real separators does not show such marked

discontinuity and its graph is similar to what is illustrated in Fig. 2.

The function $\varepsilon(\rho)$ is the main feature of the separator; knowing $\varepsilon(\rho)$ and the distribution probability, $\gamma(\rho)$ one can predict the concentrations of the useful mineral in the concentrate and the gangue in the tailings. The other parameters necessary to evaluate the effectiveness of the beneficiation can also be estimated.

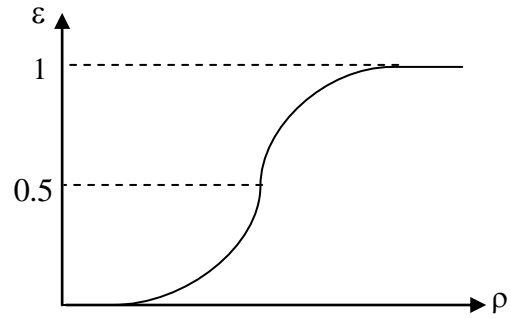


Fig. 2 Real Separation

In addition to the distribution function $\gamma(\rho)$, it is necessary to know the distribution of a useful component in the initial ore. It can be assumed that the useful component content β is a function of ρ , that is, it depends on this physical property. Actually, if the content did not depend on the ρ , beneficiation process for the classification of the particles according to the value of ρ would not guarantee obtaining populations with different concentrations of the useful component.

The percentage of particles that pass to the concentrate with respect to the total mass is expressed in Equation (3) as:

$$\bar{\gamma}_{conc} = 100 \int_{\rho_{\min}}^{\rho_{\max}} \gamma(\rho) \varepsilon(\rho) d\rho \quad (3)$$

Whilst the percentage that passes to the tailing is shown in Equation (4):

$$\bar{\gamma}_{tail} = 100 \int_{\rho_{\min}}^{\rho_{\max}} \gamma(\rho) (1 - \varepsilon(\rho)) d\rho \quad (4)$$

The concentrations of the useful components in the feed and tailings are obtained through Equations (5) to (7):

$$\bar{\beta}_{inic} = \int_{\rho_{\min}}^{\rho_{\max}} \beta(\rho) \gamma(\rho) d\rho \quad (5)$$

$$\bar{\beta}_{conc} = \frac{100}{\bar{\gamma}_{conc}} \int_{\rho_{min}}^{\rho_{max}} \beta(\rho) \varepsilon(\rho) \gamma(\rho) d\rho \quad (6)$$

$$\bar{\beta}_{conc} = \frac{100}{\bar{\gamma}_{conc}} \int_{\rho_{min}}^{\rho_{max}} \beta(\rho) (1 - \varepsilon(\rho)) \gamma(\rho) d\rho \quad (7)$$

The meaning of these equations is clear if one considers that the term $\gamma(\rho)d\rho$ is equal to the proportion of mass of the fraction of particles $[\rho, \rho + d\rho]$ of the feed ore in the separator. The value $\varepsilon(\rho)\gamma(\rho)d\rho$ is equal to the proportion of the fraction $[\rho, \rho + d\rho]$ that passed to the concentrate. The sum of these proportions is equivalent to the amount of all the concentrate with respect to the feed ore, the multiplication by 100 allows for expressing this value in percent. The values $\beta(\rho)\gamma(\rho)d\rho$ and $\varepsilon(\rho)\gamma(\rho)\beta(\rho)d\rho$ are equal to the mass of the useful component of the fraction $[\rho, \rho + d\rho]$ in the feed and in the concentrate respectively. The sum through all the possible fractions expresses the mass of the useful component in the whole concentrate; division by the yield $\bar{\gamma}_{conc}$ allows to find the average value of the concentrate $\bar{\beta}_{conc}$. In this way, the starting parameters are the fractions $\beta(\rho)$ and $\gamma(\rho)$ that characterise the particles of the feed ore due to their physical properties and the content of the useful component. These values of $\varepsilon(\rho)$, which is the main characteristic of the beneficiation, allow to calculate the usual indices of beneficiation: yield ($\bar{\gamma}_{conc}$), content ($\bar{\beta}_{conc}$) and recovery ($\bar{\varepsilon}_{conc}$). In practice, the feed is commonly divided into a finite number of fractions or classes; so the functions $\varepsilon(\rho)$, $\beta(\rho)$ and $\gamma(\rho)$ have a stepped character and the integrals that appear in the equations for the calculation of $\bar{\gamma}_{conc}$, $\bar{\beta}_{conc}$, $\bar{\beta}_{conc}$ and $\bar{\beta}_{tail}$ can be substituted with summations over the number of classes or fractions.

In the beneficiation of ores, the particles of the feed are separated by density and also by other physical properties: magnetic susceptibility (χ_m), by its specific electric charge (q), by its size (l), buoyancy (k) and its fluorescent capacity (ρ). The fundamental affirmations of the theory of separation, (presented in the form of some analyses and mathematical formula) must be, common and precise for any process of beneficiation. That is why the physical properties (ρ, l, χ, q, k) will be indicated as a common symbol (ξ), then the formulas for calculating $\bar{\gamma}_{conc}$, $\bar{\beta}_{conc}$ and $\bar{\varepsilon}_{conc}$, will be presented in Equations (8), (9) and (10) as:

$$\bar{\gamma}_{conc} = 100 \int_{\xi_{min}}^{\xi_s} \gamma(\xi) d\xi \quad (8)$$

$$\bar{\beta}_{conc} = \frac{100}{\bar{\gamma}_{conc}} \int_{\xi_{min}}^{\xi_s} \beta(\xi) \gamma(\xi) d\xi \quad (9)$$

$$\bar{\varepsilon}_{conc} = \frac{\bar{\gamma}_{conc} \times \bar{\beta}_{conc}}{\bar{\beta}_{conc}} \quad (10)$$

If the separation process considers more than one physical property or factor, it is expressed by a vector $(\xi_1, \xi_2, \dots, \xi_n)$ of \mathfrak{R}^n , the corresponding formulas would then be (Equations (11) to (14)):

$$\bar{\gamma}_{conc} = 100 \iiint \dots \int \gamma(\xi_1, \dots, \xi_n) \varepsilon(\xi_1, \dots, \xi_n) d\xi_1, \dots, d\xi_n \quad (11)$$

$$\bar{\beta}_{conc} = \iiint \dots \int \beta(\xi_1, \dots, \xi_n) \gamma(\xi_1, \dots, \xi_n) d\xi_1, \dots, d\xi_n \quad (12)$$

$$\bar{\beta}_{conc} = \left(\frac{100}{\bar{\gamma}_{conc}} \iiint \dots \int \beta(\xi_1, \dots, \xi_n) \varepsilon(\xi_1, \dots, \xi_n) \gamma(\xi_1, \dots, \xi_n) d\xi_1, \dots, d\xi_n \right) \quad (13)$$

$$\bar{\beta}_{tail} = \left(\frac{100}{\bar{\gamma}_{conc}} \iiint \dots \int \beta(\xi_1, \dots, \xi_n) [1 - \varepsilon(\xi_1, \dots, \xi_n)] \gamma(\xi_1, \dots, \xi_n) d\xi_1, \dots, d\xi_n \right) \quad (14)$$

where the region of integration is the region of allowable values of the vector $(\xi_1, \xi_2, \dots, \xi_n)$. In this case, generalised equations can be expressed in Equations (15) and (16) as:

$$\bar{\gamma}_{conc} = 100 \int_{\xi_{min}}^{\xi_s} \gamma(\xi) \varepsilon_{conc}(\xi) d\xi \quad (15)$$

$$\approx 100 \sum_{i=1}^n \gamma(\xi_i) \varepsilon_{conc}(\xi_i) \Delta \xi_i$$

$$\bar{\beta}_{conc} = \frac{100}{\bar{\gamma}_{conc}} \int_{\xi_{min}}^{\xi_s} \beta(\xi) \gamma(\xi) \varepsilon_{conc}(\xi) d\xi$$

$$\approx \frac{100}{\bar{\gamma}_{conc}} \sum_{i=1}^n \beta(\xi_i) \gamma(\xi_i) \varepsilon_{conc}(\xi_i) \Delta \xi_i \quad (16)$$

In the same way, in Equations (15) and (16), the number $\gamma(\xi)d\xi$ is equivalent to the portion (mass) of the narrow fraction of the particles $[\xi, \xi + d\xi]$ of the feed in the beneficiation equipment, and the number $\gamma(\xi)\varepsilon_{conc}(\xi)d\xi$ equals the part of the fraction $[\xi, \xi + d\xi]$ which passes to the concentrate. The sum of these fractions represents the part of the total in the concentrate in comparison with the initial feed, and multiplication by 100 allows to determine the output of the concentrate in percent. The numbers $\gamma(\xi)\beta(\xi)d\xi$ and $\beta(\xi)\gamma(\xi)\varepsilon_{conc}(\xi)d\xi$ are equal to the mass of the component of the metal of interest, in the corresponding narrow fraction $[\xi, \xi + d\xi]$ of the unit of mass (1 kg) in the feed and in concentrate.

The sum of all the fractions represents the mass of the useful component in the concentrate. The division by the yield of the concentrate $\bar{\gamma}_{conc}$ allows to calculate the average content of the mineral of interest in the concentrate $\bar{\beta}_{conc}$. The tailings formula in Equation (17) are analogous with a difference.

$$\varepsilon_{tail}(\xi) = 1 - \varepsilon_{conc}(\xi). \quad (17)$$

In this way, the initial functions are $\gamma(\xi)$ and $\beta(\xi)$ which in turn characterise the particles of the feed, and the function $\varepsilon_{conc}(\xi)$ is the fundamental separation characteristics of the beneficiation apparatus (Tikhonov, 1978, 1984.). For the typical parameters of beneficiation: yield ($\bar{\gamma}_{conc}$), grade ($\bar{\beta}_{conc}$) and recovery ($\bar{\varepsilon}_{conc}$), a script is placed on these numbers to differentiate them from the functions. The works of Hernández (1997, 2000); Coello *et al.* (1998); Ramírez (2002); (Agyei *et al.* (2010); Agyei and Beyris (2011) and Hernandez *et al.* (2017) demonstrate the feasibility of this method for laterite ore because of the diversity of minerals present whose particles are bearers of different elements and differentiated by several physical properties. The differential functions of mass and content distributions, $\gamma(\xi)$ and $\beta(\xi)$, are a simple and sufficient means for the characterisation of any raw material or product. These functions not only permit the calculation of the classic beneficiation indicators, but also contribute to the prediction of the technological indices of any beneficiation flowsheet, independent of the separation property.

2 Resources and Methods Used

The materials used were selected from sample pits 44 and 45 of block M-49 of the Punta Gorda deposit. A technological sample composed of oxidised nickel ore was prepared. The sampling of the technological sample was made on the exploitation face from the bottom to the uppermost levels, which cover sample pits 44 and 45 with thickness of 35.1 and 24 m respectively. The sample with a mass of approximately 1400 kg was passed through homogenisation and quartering.

Chemical analysis was done using X-Ray Fluorescence Phillips PW 1480, using an Rn radiation type PW2182 / 00, under processing regime of 3000 W and 100 KV vacuum with fine collimator. X-ray Powder Diffraction was conducted using the polycrystalline method with a diffractometer type HZG-4 with C radiation, under processing conditions of 30 KV, 20 mA, 2 θ , 5 to

80° and voltage generator TUR M-62) was used. For the registration and treatment of the roentgenometric data, the ANALIZE and AUTOQUAN software, of the SEIFERT X - Ray Technology (Version 2.26), were used.

The balance laterite of Punta Gorda deposit is essentially ferrous, with a head grade iron content of approximately 47%, as shown in Table 1. The size analysis constitutes one of the fundamental stages for the characterisation of the ore under study. In its characterization, wet screening was used following Tyler series in particle sizes that range between 8 and 0.044 mm, considering similar works by Mitrofanov *et al.*, (1982); Falcón and Hernandez, (1993); Falcon *et al.*, (1997a, 1997b); Hernández, (1997); Coello *et al.*, (1998) and Ramírez, (2002).

Table 1 Head Grade Analysis of the Ore from Punta Gorda

Element	Content (%)
Ni	1.34
Co	0.134
Fe	46.928
Mn	0.42
Mg	3.69
Cr	3.18
Al	2
SiO ₂	0.92
Cu	0.019
Zn	0.037

The dry magnetic analysis was carried out in the Mineral Beneficiation Laboratory of Instituto Superior Minero Metalurgico (ISMM) of Moa. The following current intensities: 0.5; 1; 2; 4 and 6 A, were applied to the following size classes: (-10 + 8) mm; (-8 + 4) mm; (-4 + 2) mm; (-2 + 1) mm, using a roller separator model 13b-C δ . The separator is suitable for the dry analysis of weak magnetic ores. The one used has a roll diameter of 100 mm and is 80 mm long; the field strength reached was 950 kA/m; and the mass is 149 kg. The external dimensions are as follows:

- (i) Length ----- 900 mm
- (ii) Width ----- 520 mm
- (iii) Height ----- 545 mm

The fine fractions: (-1.0 + 0.4) mm; (-0.4 + 0.2) mm; (-0.2 + 0.071) mm; (-0.071 + 0.044) mm and - 0.044 mm were analysed through wet screening process in a Davis Tube Tester in the Nickel Research Centre and in the ISMM of Cuba.

3 Results and Discussion

3.1. Determination of the Fractional Distribution

The results of the size analysis and magnetic analysis as well as the chemical composition of the nickel ore studied are presented in this section. The functions of mass and content distribution are analysed using the aforementioned properties. From the size analysis, the nickeliferous ore is composed of particles smaller than 0.071 mm, reaching 76.58% by weight of the sample. Goethite constitutes the predominant mineral phase followed by hematite, gibbsite, chromite and minerals of the serpentine group corroborating with Almaguer (1993, 1996); Rojas (1995) and Agyei, (2006) as shown in Table 2.

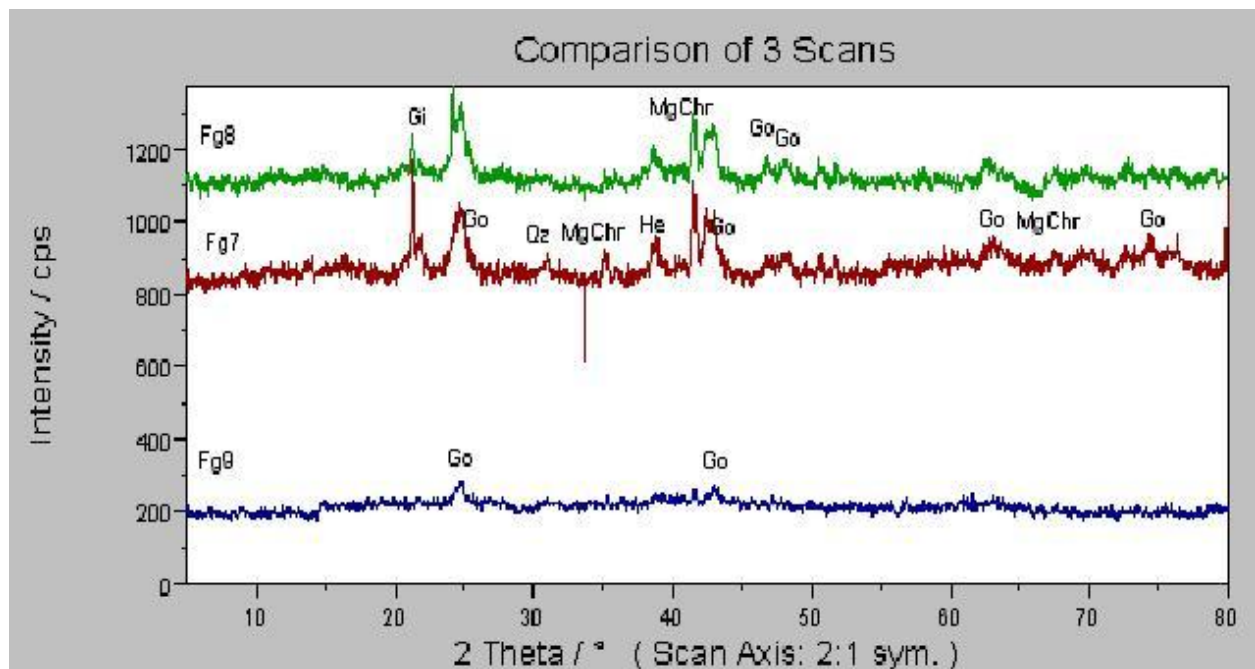
By the study of X-ray Diffraction, it was possible to detect more than one type of goethite, apparently with a different degree of crystallinity, indicating that there is a process of alteration of the Fe oxides in the lateritic profile, reflected in the paragenesis of goethite and hematite (Fig. 3). All this allows one to suppose a process of continuous weathering

that gives rise to phases of Fe, and Mn, which can be bearers of Ni and Co (Almaguer, 1989). In this lateritic nickel ore, a marked regularity of distribution was revealed for the following: SiO₂, Al, Mg, and Fe and this corroborate with (Agatzini *et al.*, 2004a; Agatzini and Safiratos, 2004b; Agyei *et al.*, 2010; and Agyei and Beyris, 2011) for similar lateritic materials.

It was possible to establish, among the mineralogical types that were fully detected by X-ray diffraction according to particle size and magnetic separations, the phases of oxides of Fe such as magnetite, maghemite, magnesiochromite, goethite and hematite. Other mineral phases detected were serpentine group minerals, iron oxides and manganese mineral phases such as asbolanes and lithiophorites (Table 2).

3.2 Analysis of the Mass Distribution According to Particle Size

The differential distribution function $\gamma(\xi)$ of the particles of any mixture with a given physical property (ξ) is that for which the product $\gamma(\xi)d\xi$ is equal to the mass fraction of any basic interval and its increment $d\xi$; the function $\gamma(\xi)$ is nothing other than the function of differential distribution density of the particles in the fractions (Tikhonov, 1984).



Legend: Go-Goethite, Gi-Gibbsite, MgChr -Magnesiochromite, He- hematite, Qz-Quartz
Size fractions: Fg7- (-0.2+0.071) mm, Fg8- (-0.071+0.44)mm, Fg9- (-0.44+0.0)mm

Fig. 3 X-ray Diffraction Analysis of the Fine fractions

Table 2 Quantitative Distribution of Mineralogical Phases of the Ore from Punta Gorda

Minerals	Size Fractions								
	-10+8	-8+4	-4+2	-2+1	-1+0.4	-0.4+0.2	0.2+0.07	-0.071+0.044	0.044
Chlorite lib-2	13.4	7.3	9.2	5.4	3.36	2.43	2.21	7.3	3.09
Gibbsite	43.99	25.141	27.22	22.9	15.7	8.9	7.6	0.4	1.67
Goethite	16	43.3	35.2	53.5	67.3	70.34	68.42	78.7	83.1
Hematite	2.7	0	3.71	1.3	1.93	2.77	3.89	0.91	4.53
Lithiophorites	4.3	3.94	4.98	4.68	3.29	3.66	6.21	1.67	0
Lizardite1T	8.66	12.96	9.89	7.82	1.41	1.43	1.22	3.88	0.58
Maghemite	1.15	0	0.84	0	5.87	6.34	2.45	0	7
Magnesiochromite	0.97	4.66	6.42	2.77	0.75	3	6.77	7.07	0.03
Magnetite	0	0.25	0.79	0	0	0	0	0	0
Quartz	8.83	2.18	1.75	1.63	0.39	1.13	1.23	0.07	0
Total	100	100	100	100	100	100	100	100	100

For the determination of the function $\gamma(l)$ in Table 3, it was necessary to first find the weight fraction of the particles within the corresponding intervals Δl and divide it by the range, Δl . The size distribution analysis of the balance laterite is shown in Table 3.

In Fig. 4, it can be seen that, 80% of the particle sizes fall below 0.071 mm. The increase in the value of the distribution function $\gamma(l)$ towards the finer fractions is shown in Table 3, corroborating the results of Falc3n *et al.* (1993); Coello *et al.* (1998); Hern3ndez *et al.* (1997, 2000) for these types of lateritic materials.

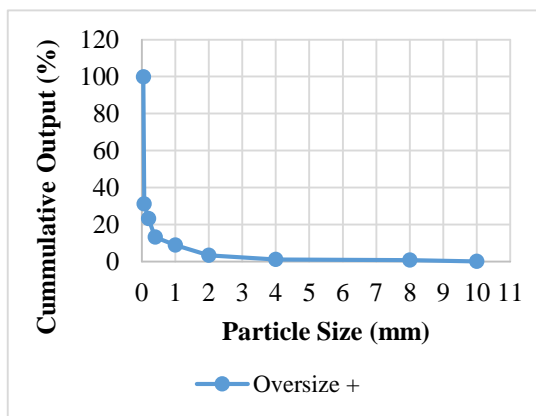


Fig. 4 Curves Summary Characteristics of Size Analysis of Punta Gorda

Equation (18) describes the mass distribution function that characterises the ore taking as property of analysis, the size of the particle whose numerical values are in Table 3.

$$\gamma(l) = \int_{l_{\min}}^{l_{\max}} (15.0351e^{-1.30631}) dl \quad (18)$$

$$R^2 = 0.9864$$

3.3 Content Distribution Function by Particle Size

The components such as Al, SiO₂, and Mg in Table 4 enrich towards the coarse fractions. However, nickel and iron accumulate in the fine fractions from 1.0 mm to 0.044 mm and these corroborate with those found by Rojas, (1995) and Agyei *et al.* (2010).

The mathematical expressions in Equations (19) to (24) describe the content distribution function using as property, the particle size. The composition of nickel describes a polynomial function towards the fine size fractions. Iron tends to increase with a lineal function towards the fines. Al, Mg, SiO₂ show exponential functions towards the coarse fractions greater than 1.0 mm whilst chrome concentrates in the intermediate fractions between 0.2 mm to 1.0 mm with typical polynomial functions.

$$\beta^{Ni}(l) = \int_{l_{\min}}^{l_{\max}} (-0.03421^2 + 0.1771 + 1.229) dl \leq 1.0 \text{ mm} \quad (19)$$

$$R^2 = 0.92$$

$$\beta^{Fe}(l) = \int_{l_{\min}}^{l_{\max}} (-3.6227l + 50) dl \quad (20)$$

$$R^2 = 0.91$$

Table 3 Experimental Results of The Punta Gorda Basic Distribution Function $\gamma(l)$

Size Classes (mm)	Average Particle Size (mm)	Class Interval Δl	Distribution Function distribution $\gamma(l)$, 1/mm	$\gamma(l) \cdot \Delta l$
-10+8	9.0	2.0	0.0005	0.0010
-8+4	6.0	4.0	0.0016	0.0063
-4+2	3.0	2.0	0.0018	0.0036
-2+1	1.5	1.0	0.0228	0.0228
-1+0.4	0.7	0.6	0.0922	0.0553
-0.4+0.2	0.3	0.2	0.2140	0.0428
-0.2+0.071	0.1355	0.129	0.7845	0.1012
0.071+0.044	0.0575	0.027	2.9259	0.0790
-0.044+0	0.022	0.044	15.6341	0.6879

Table 4 Experimental Function of the $\beta(l)$ Content of Punta Gorda

Size Classes (mm)	Average Particle Size	Chemical Composition, %							
		Ni	Co	Fe	Mn	Mg	Cr	Al	SiO ₂
-10+8	9.0	1.80	0.365	20.69	3.08	5.67	0.27	12.76	20.16
-8+4	6.0	1.56	0.229	21.85	2.18	5.54	0.23	9.83	22.16
-4+2	3.0	1.60	0.323	22.18	2.72	5.92	0.27	9.62	19.38
-2+1	1.5	1.08	0.225	34.63	1.71	1.87	1.30	5.32	6.71
-1+0.4	0.7	1.20	0.264	39.20	1.84	1.08	2.11	4.15	4.43
-0.4+0.2	0.3	1.42	0.404	36.50	2.98	0.79	2.09	4.10	3.94
-0.2+0.071	0.14	1.50	0.349	38.91	2.57	0.70	2.37	3.65	4.01
0.071+0.044	0.06	1.40	0.192	43.90	1.40	0.57	2.68	3.44	3.75
-0.044+0	0.022	1.38	0.092	49.66	0.63	0.43	1.96	3.51	3.41

$$\beta(l)^{Cr} = \int_{l_{min}}^{l_{max}} (0.16161^{-1.296}) dl \quad (22)$$

$R^2 = 0.90$

$$\beta(l)^{Al} = \int_{l_{min}}^{l_{max}} (3.275e^{0.17521}) dl \quad (23)$$

$R^2 = 0.95$

$$\beta(l)^{SiO_2} = \int_{l_{min}}^{l_{max}} (4.54e^{0.26871}) dl \quad (24)$$

$R^2 = 0.85$

These results are corroborated through the coefficient of correlations calculated, with respect to the analysis of variance, and in all cases, the Fisher calculated is greater than the critical Fisher with probability greater than 0.05, which demonstrates the reproducibility of the models obtained.

3.4 Mass Distribution According to Magnetic Analysis

The functions increase from 1 A to 2 A, where they reach maximum points, and then decrease. For fractions larger than 1.0 mm, the distribution function increases from 0.5 to 4 A and then decreases towards high intensities. This could be explained by relatively low content of paramagnetic particles in the coarse fractions. Equations (25) to (33) highlight the mass distribution of the ore taking as property, the current intensity of the analyser.

$$\gamma^{-0.044mm}(I) = \int_{I_{\min}}^{I_{\max}} (0.0003I^4 - 0.004I^3 + 0.0216I^2 - 0.0375I + 0.0198) dI \quad (25)$$

$$R^2 = 0.99$$

$$\gamma^{+0.044mm}(I) = \int_{I_{\min}}^{I_{\max}} (0.0093I^4 - 0.1109I^3 + 0.4458I^2 - 0.6792I + 0.335) dI \quad (26)$$

$$R^2 = 0.99$$

$$\gamma^{+0.071mm}(I) = \int_{I_{\min}}^{I_{\max}} (0.0151I^4 - 0.1845I^3 + 0.7641I^2 - 1.2239I + 0.6291) dI \quad (27)$$

$$R^2 = 0.99$$

$$\gamma^{+0.2mm}(I) = \int_{I_{\min}}^{I_{\max}} (0.0091I^4 - 0.1096I^3 + 0.445I^2 - 0.6898I + 0.3453) dI \quad (28)$$

$$R^2 = 0.99$$

$$\gamma^{+0.4mm}(I) = \int_{I_{\min}}^{I_{\max}} (0.0105I^4 - 0.1289I^3 + 0.5368I^2 - 0.8668I + 0.4478) dI \quad (29)$$

$$R^2 = 0.99$$

$$\gamma^{+1.0mm}(I) = \int_{I_{\min}}^{I_{\max}} (-0.0059I^4 + 0.0794I^3 - 0.3514I^2 + 0.4828I + 0.1778) dI \quad (30)$$

$$R^2 = 0.99$$

$$\gamma^{+2.0mm}(I) = \int_{I_{\min}}^{I_{\max}} (-0.0104I^4 + 0.1321I^3 - 0.5583I^2 + 0.8135I - 0.0675) dI \quad (31)$$

$$R^2 = 0.99$$

$$\gamma^{+4.0mm}(I) = \int_{I_{\min}}^{I_{\max}} (-0.0043I^4 + 0.0584I^3 - 0.2623I^2 + 0.3994I + 0.0048) dI \quad (32)$$

$$R^2 = 0.99$$

$$\gamma^{+8.0mm}(I) = \int_{I_{\min}}^{I_{\max}} (-0.0039I^4 + 0.053I^3 - 0.2376I^2 + 0.354I + 0.0305) dI \quad (33)$$

$$R^2 = 0.99$$

3.5 Bidimensional Distribution based on Size and Current Intensity in Magnetic Analyser

For the determination of the function $\gamma(l, I)$ in Table 5, it was necessary to first find the weight fraction of the particles within the corresponding

intervals Δl and ΔI divide it by the range of the interval Δl and ΔI as indicated by Equation (34):

$$\gamma(l, I) = \frac{\gamma(l)\gamma(I)}{\Delta l \times \Delta I} \quad (34)$$

The equations (35) to (41) describe the joint content distribution of the ore taking into consideration, the magnetic susceptibility and the size.

$$\beta(l, I)^{Ni} = \int_{I_{\min}}^{I_{\max}} \int_{l_{\min}}^{l_{\max}} [(-0.0342I^2 + 0.177I + 1.229) \times (0.2797I + 0.9288)] dldI \quad (35)$$

$$R_l^2 = 0.92; R_I^2 = 0.94$$

$$\beta^{Co}(l, I) = \int_{I_{\min}}^{I_{\max}} \int_{l_{\min}}^{l_{\max}} (0.6351e^{-0.2654}) dldI \quad (36)$$

$$R^2 = 0.89$$

$$\beta^{Fe}(l, I) = \int_{I_{\min}}^{I_{\max}} \int_{l_{\min}}^{l_{\max}} [(-3.6227I + 50)((30 - 50)e^{-0.1099I})] dldI \quad (37)$$

$$R_l^2 = 0.91; R_I^2 = 0.80$$

$$\beta(l, I)^{Mg} = \int_{l_{\min}}^{l_{\max}} \int_{I_{\min}}^{I_{\max}} \left[\left((0.8 - 2)e^{0.37161} \right) \left((2 - 5.41)e^{0.07121} \right) \right] dl dI \quad (38)$$

$$R_l^2 = 0.92; R_I^2 = 0.89$$

$$\beta(l, I)^{Cr} = \int_{l_{\min}}^{l_{\max}} \int_{I_{\min}}^{I_{\max}} \left[\left(0.1616l^{-1.296} \right) \left((6.38 - 9.25)e^{0.07121} \right) \right] dl dI \quad (39)$$

$$R_l^2 = 0.90; R_I^2 = 0.80$$

$$\beta(l, I)^{Al} = \int_{l_{\min}}^{l_{\max}} \int_{I_{\min}}^{I_{\max}} \left[\left(3.275e^{0.17521} \right) \left((1.2 - 6.42)e^{0.10791} \right) \right] dl dI \quad (40)$$

$$R_l^2 = 0.95; R_I^2 = 0.98$$

$$\beta(l, I)^{SiO_2} = \int_{l_{\min}}^{l_{\max}} \int_{I_{\min}}^{I_{\max}} \left[\left(4.5e^{0.26871} \right) \left((1.2 - 15)e^{0.12481} \right) \right] dl dI \quad (41)$$

$$R_l^2 = 0.85; R_I^2 = 0.86$$

Table 5 Experimental Results of the Mass Distribution Function $\gamma(l, I)$ from Punta Gorda

Size (mm)	Values of the Joint Distribution Function, (mm. A)				
	(I), A				
	0.0-0.5	0.5-1.0	1.0-2.0	2.0-4	4.0-6.0
-10+8.0	0.00010	0.0001	0.0000	0.0000	0.0000
-8.0+4	0.0003	0.0002	0.0001	0.0001	0.0000
-4.0+2.0	0.0001	0.0004	0.0001	0.0001	0.0001
-2.0+1.0	0.0087	0.0063	0.0029	0.0013	0.0008
-1.0+0.2	0.0000	0.0000	0.0049	0.0018	0.0007
-0.4+0.2	0.0000	0.0031	0.0128	0.0055	0.0044
-0.2+0.071	0.0000	0.0032	0.0623	0.0213	0.0092
-0.071+0.044	0.0000	0.0612	0.1923	0.0712	0.0263
-0.044+0.00	0.0000	0.00000	0.1530	0.2166	0.1627

These results can be further be corroborated through the statistical analysis, which is generally seen to have coefficients of correlations greater than 0.80 in all cases. In addition, the Fisher value calculated is less than the critical Fisher which shows the reproducibility of the obtained models.

4 Conclusions

The regularities of the differential mass and content distribution and the content of the phases and metallic species present in the Cuban nickel oxide ore were obtained considering the size of the mineral particles and magnetic susceptibility and their combinations. These results may add up to the new knowledge about the possibilities of pre-concentration of the components which in effect, would help to improve the quality of the ochreous nickel laterite supplied to the extractive process. The integral-differential equations and their joint mass and content distribution functions for the nickel ore for the Caron process were determined, taking as properties of analysis the size, and magnetic susceptibility that describe the distribution of Ni, Fe, SiO₂, Al, Mg, and Cr.

References

- Agatzini, S. L., Safiratos, I. G. and Spathis, D. (2004a.), "Beneficiation of a Greek Serpentinic Nickeliferous Ore Part I", *Hydrometallurgy*, Vol. 74, No. 3-4, pp. 259 – 265.
- Agatzini, S. L. and Safiratos, I. Z. (2004b), "Beneficiation of a Greek Serpentinic Nickeliferous Ore. Part II. Sulphuric Acid Heap and Agitation Leaching", *Hydrometallurgy*, Vol. 74, No. 3–4, pp. 267 – 275.
- Agyei, G. (2006), "Distribución Fraccional de las Especies Metálicas y Mineralógicas de la Mena Niquelífera de un Perfil del Yacimiento Punta Gorda, Moa, Cuba", *Unpublished PhD Thesis*, Instituto Superior Minero Metalúrgico Moa, Cuba. 92 pp.
- Agyei, G., Rojas, A. L. and Hernández, A. (2010), "Distribución Fraccional de Metales y Minerales en la Laterita de Balance del Yacimiento Punta Gorda, Moa, Cuba", *Minería & Geología*, Vol. 26, No. 4, pp. 36 – 52.
- Agyei, G. and Beyris, P. E. (2011), "Modelación de la Distribución Fraccional Magnética de la

- Mena Oxidada Niquelífera”, *Minería y Geología*, Vol. 27, No. 4, pp. 40–63.
- Almaguer A. F. and Zamarsky, V. (1993), “Estudio de la Distribución del Fe, Ni y Co en los Tamaños de Granos que Componen el Perfil de las Cortezas de Intemperismo de las Rocas Ultrabásicas hasta su Desarrollo Laterítico y su Relación con la Mineralogía”, *Minería y Geología*, Vol. 1, No. 1, pp. 17–24.
- Almaguer, A. F. (1996), “Composición de las Pulpas Limonititas de la Planta Pedro Sotto Alba Parte II-Periodo de Crisis de Sedimentación” *Minería y Geología*. Vol. 13. No.1, pp. 27–30.
- Almaguer, A. F. (1995), “Cortezas de Intemperismo: Algunas Características de sus Partículas Finas”, *Minería y Geología*, Vol.1 No. 1, pp. 9–19.
- Almaguer, A. F. (1989), “Mineralogía y Geoquímica de las Cortezas de Intemperismo Lateríticas de las Rocas Ultramafitas de la Provincia Holguín”. *Unpublished PhD Thesis*, Technical University of Ostrava, 97 pp.
- Beyris, P. E (1997). “Mejoramiento del Proceso de Sedimentación de la Pulpa del Mineral Laterítico de la Empresa Pedro Sotto Alba, Moa Nickel S.A”, *Unpublished PhD Thesis*, ISMM, Moa, Cuba, 118 pp.
- Carthy, G. C. and Falcon, J. (1985), “Consideraciones Preliminares sobre el Beneficio de las Colas de Nicaro”, *Minería y Geología*, Vol. 2, No. 8, pp. 124–131.
- Coello, A. L., Beyris, P. E., Hernández, A. and Ramírez, B. (1998), “Distribución Fraccional de los Valores Metálicos en el Escombro Laterítico”, *Minería y Geología*, Vol. 15 No. 1, pp 37–42.
- Falcón, J., Beyris, P. E., Ferrer, E. A. and Montero, M. (1997a), “Sedimentación de la Pulpa Cruda en la Empresa Moa Níquel S.A”, *Minería y Geología*, Vol. 14, No. 1, pp. 31–36.
- Falcón, J. Hernandez, A. and Coello, A. L. (1997b), “Preparación Mecánica de los Minerales Lateríticos”, *Revista Tecnológica*, Vol. 1, No. 1, pp. 9–17.
- Falcón, J., Hernández, A. (1993), Preparación y Beneficio de Minerales Lateríticos en el Proceso Acido a Presión”, *Minería y Geología*, Vol. 2, No.2, pp. 51–58.
- Hernández, A., Agyei G. and Rojas, A. L. (2017), “Estudio Fraccional Densométrico de la Mena Laterítica: Evaluación del Enriquecimiento”, *Minería & Geología*, Vol. 33, No. 3, pp. 293–311.
- Hernández, A., Falcón J., Trujillo, R. and Toirac, M. (2000), “Análisis Teórico del Beneficio de la Laterita”, *Revista Minería y Geología*, Vol. 17, No. 3–4, pp. 73–78.
- Hernández, A., Toirac, M. and Coello, A.L. (1995), “Estudio Preliminar para la Obtención de Concentrados de Cromo a partir del Yacimiento de Cortezas de Intemperismo Casimba Pinares de Mayari”, *Minería y Geología*, Vol. 12, No 2, pp. 23–26.
- Hernandez, A. (1997), “Determinación de Esquemas Racionales para la Preparación y Beneficio Integral de Minerales Lateríticos”, *Unpublished PhD Thesis*, ISMM, Moa, Cuba, 94 pp.
- King, R. P. (2001), *Modelling and Simulation of Mineral Processing Systems*, Butterworth Heinemann, 402 pp.
- Leyva, E. R., Rodríguez, J. E. G. and Jesús-Ortiz, J. B. (1995), “Contribución al Estudio Estructural de los Minerales Componentes de las Colas de Nicaro”, *Minería y Geología*, Vol. 12, No. 2, pp. 9–15.
- Mitrofanov, L. A, Borski, V. D. and Samygin, (1982), *Investigación de la Capacidad de Enriquecimiento de los Minerales*, Editorial Mir, Moscú, 439 pp.
- Ponce, N. and Carrillo, D. (1984), “Mineralogía y Composición Sustancial de las Menas Ferro-niquelífera del Yacimiento Delta, Moa”, *Serie Geológica*, No. 3, pp. 3–16.
- Ponce, N. and Carrillo, D. (1988), “Mineralogía y Composición Sustancial de las Muestras Patrones de Lateritas” *Serie Geológica*, No. 1, pp. 75 – 82.
- Ramírez, M. (2002), “Estudio de Beneficiabilidad de los Escombros Lateríticos de la Región Moa”, *Unpublished MSc Thesis*, ISMM, Moa, Cuba, 54 pp.
- Rodríguez C, A. (1990), “Prospección y Exploración de las Cortezas de Intemperismo sobre Ultramafitas en Nicaro y Pinares de Mayari”. *Unpublished PhD Thesis*, ISMM, 98 pp.
- Rojas, A. L. (1995), “Principales Fases Minerales Portadores de Níquel en los Horizontes Lateríticos”, *Unpublished PhD Thesis*, ISMM, Moa, Cuba, 75 pp.
- Rojas, A. L. and Beyris, P. E. (1994), “Influencia de la Composición Mineralogica del Material Limonítico de Frentes de Explotación de la Industria Pedro Sotto Alba, Moa,” *Minería y Geología*, Vol. 11, No. 1, pp. 13–17.
- Tikhonov, O. N. (1984) *Regularities of effective separation of minerals in processes of mineral enrichment*, Nedra, Moscow, 316 pp.
- Tikhonov, O. N. (1978), *Fundamentos Teóricos de Procesos de Separación en la Concentración de Minerales*, Edición Nedra, San Petersburgo, Rusia, 412 pp
- Vera, A. Y. (1979), *Introducción a los Yacimientos de Níquel Cubanos*, La Habana, Editorial Orbe, 213 pp.

Authors



George Agyei is a Senior Lecturer currently working at the University of Mines and Technology, Tarkwa. He holds BSc and PhD degrees from Instituto Superior Minero Metalurgico de Moa, Cuba. He also holds an MBA from Educatis University, Altdorf, Switzerland. He is a member of Institute of Quarry, UK and WAIMM. His research and consultancy works cover Ore Beneficiation, Process Mineralogy, Sustainability and Mining



Alberto Hernandez Flores is a Professor of Metallurgical Engineering and a Consulting Engineer currently working at the Instituto Superior Minero Metalurgico de Moa, Cuba. He is a Principal Researcher at the Cuban Centre for Chemical Research. He holds degrees of MSc and PhD from the Instituto Superior Minero Metalurgico de Moa, Cuba. His research and consultancy works cover Mineral Processing, Fertilizers, Pigments, Pedagogy and Management.



Arturo Rojas Purón is a Professor of Geology and a Consulting Engineer currently working at the Instituto Superior Minero Metalurgico de Moa. He holds MSc and PhD degrees from the Instituto Superior Minero Metalurgico de Moa. He is a member of the Geological Society of Cuba. His research and consultancy works cover Mineralogy, Environmental, Geology and Nanotechnology.